

# 55 MEV RACE-TRACK MICROTRON OF LEBEDEV INSTITUTE

A.I.Karev, A.N.Lebeдев, V.G.Raevsky#, P.N.Lebeдев Physical Institute, RAS, 119991, Moscow, Russia

A.N.Kamanin, N.I.Pakhomov, V.I.Shvedunov, SINP MSU, 119992, Moscow Russia.

## Abstract

The design of 55 MeV Race-Track Microtron (RTM) with pulse current up to 50 mA has been completed and now accelerator is under construction. We present the general scheme of this microtron, the basic results of computer simulation, the parameters of the RTM components and describe engineering design and status of the machine.

## INTRODUCTION

55 MeV RTM is under construction at Lebedev Physical Institute RAS. The main parameters of RTM are given in Table 1 and the general scheme of the machine is shown in Fig.1.

Table 1: RTM parameters

Output energy	55 MeV
Output pulse current	up to 50 mA
Number of linac passages	11
Energy gain / turn	5 MeV
Pulse length	up to 15 $\mu$ s
Operating frequency	2.856 MHz
End magnet field	1.0 T
Klystron power pulsed	6 MW
Orbit circumference increase / turn	1 $\lambda$

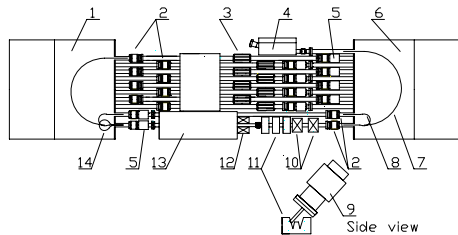


Figure 1: RTM schematic.

The electron beam from the 50 keV gun (9) is injected from the top into the linac (13) through the injector magnet (11) and solenoidal lens (12). After acceleration in the linac 5 MeV electrons are reflected back on its axis via trajectory (14) by the special fringe field configuration of the end magnet (1). As the linac operates in a standing wave mode, after the second passage through the accelerating structure in the reverse direction the beam energy is doubled and trajectory (8) radius in the second end magnet (6) becomes sufficient to bypass accelerating structure cavities through the hole drilled in the linac wall. The 55 MeV beam (7) is extracted from the RTM

# raevsky@venus.lpi.troitsk.ru

with magnet (4). The quadrupole doublet (10) on the linac axis provides beam focusing. Beam current monitors (BCM) (5) are used to control pulsed beam current at orbits and steering coils (3) to adjust beam trajectory. Bellows which are part of BCMS together with bellows (2) permit to move both end magnets along the linac axis.

## COMPUTER SIMULATION

### End magnet

The end magnet schematic cut view is shown in Fig. 2(a). It consists of the yoke (1), the main poles (2) with coils (3), the reverse field poles (4) with coils (5), the active screen (6) with coils (7) and passive screen (8). The pole gap height is 2 cm, the project median plane field in the main poles region is 1 T.

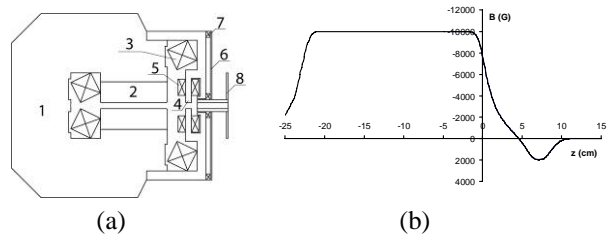


Figure 2: End magnet cut view (a) and median plane field (b).

The end magnet optimization with 2D and 3D codes was done using real steel permeability. To reach operating field level 1T with uniformity better than 0.1% in the region of main poles 0.3 mm air gap was introduced between the main poles and the yoke. The fringe field was optimized to provide 5 MeV beam trajectory closer with reasonable focusing properties: at 5 MeV end magnet focuses beam with focal power  $-1.6 \text{ m}^{-1}$ , while at 10 MeV and at higher energies it acts as defocusing lens with focal power decreasing as energy squared from  $0.1 \text{ m}^{-1}$ . Resulting median plane end magnet field distribution including fringe field zone is shown in Fig. 2.

### Accelerating structure

A standing wave bi-periodic on-axis coupled accelerating structure with  $\pi/2$  operating mode at 2856 MHz was chosen for the RTM linac [1]. Schematic view of the linac is illustrated in Fig.3. Linac consists of 7 accelerating A1-A7 and of 6 coupling cells C1-C6. To effectively accelerate the low-energy beam from the gun and the high-energy beams at the orbits the 1<sup>st</sup> cell has  $\beta = 0.7$ , and the rest cells have  $\beta \approx 1$ . The effective shunt impedance and the coupling factor of  $\beta \approx 1$  cells are, correspondently, 82 MOMh/m and 6.1 %. The dimensions

of the coupling slot in feeding waveguide were adjusted to get coupling coefficient with linac 4.3 which provides zero reflected wave at total beam current loading from all RTM orbits equal 750 mA.

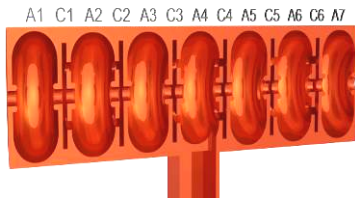


Figure 3: RTM accelerating structure.

### Electron gun and injection magnet

Taking into account maximum project beam current at RTM exit and expected RTM capture efficiency, 400 mA nominal current was chosen for the electron gun operating at -50 kV cathode voltage. Regulation of the injected beam current within  $\pm 100$  mA with small beam dimensions variation can be done by regulation of the intermediate anode voltage.

The injection magnets system is shown in Fig. 4. To compensate higher orbits deflection by injection magnet M1 we included in the system two additional magnets, M2 and M3, the coils of all three magnets are connected in series and are fed from a single source. The magnets system is mirror symmetric with respect to M2 centre, the angle of the pole face rotation for M1 magnet was adjusted taking into account 3D effects to provide optimal 50 keV beam focusing.

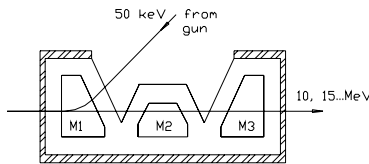


Figure 4: Injection magnets system.

### RTM beam dynamics

Using the end magnet and linac field distributions we simulated beam dynamics in RTM [2] with RTMTRACE code [3]. The goals of simulation were (1) fixing of the field settings for the end magnets, the accelerating structure and the quadrupoles; (2) fixing elements position with respect to each other; (3) calculations of the beam trajectories for all RTM orbits; (4) estimation of the RF power dissipated in the linac and beam power losses; and (5) estimation of the beam parameters at RTM exit.

Table 2: Output beam parameters

Beam energy (MeV)	55.5
Energy spread (keV)	83.9
Hor./vert. norm. emittance (mm x mrad)	9.7/27.5
Hor./vert. beam size (mm)	1.7/1.7
Bunch length (degree)	4.5

Output beam parameters are summarized in the Table 2. For optimally tuned RTM at  $16^\circ$  synchronous phase  $\sim 16\%$  of the injected electrons are accelerated to  $\sim 55$  MeV. The main beam losses take place at the 1<sup>st</sup> and 2<sup>nd</sup> orbits, total beam losses till the last orbit are  $\sim 0.4$  MW. The RF power losses till the last orbit are  $\sim 1.1$  MW. Thus, with 6 MW klystron more than 60 mA pulsed current could be obtained at RTM exit.

### ENGINEERING DESIGN

The RTM assembly drawing is shown in Fig. 5. All RTM elements are fixed on a common frame (12) with central table (3) at which the electron gun (4), the linac (2), and other elements are installed, and movable side tables (7) for the end magnets (1, 5). The klystron (11) is fixed at adjustable table (10) inside the frame. Below description of some elements and systems is given.

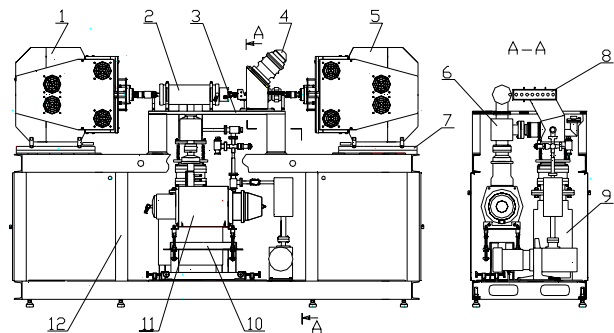


Figure 5: RTM assembly drawing.

The end magnets are made of high quality magnetic steel. To provide field uniformity  $\sim 0.1\%$  the distance between the main poles is kept constant with accuracy  $\pm 0.01$  mm by special spacers, the assembly of two poles is inserted inside the yoke with air gaps 0.3 mm at the top and bottom of assembly. The coils of the main and reverse field poles are cooled by water via copper plates inserted in coils and by fans.

The linac cells are made of OFHC copper and are brazed by silver alloy in the hydrogen atmosphere furnace. Linac is cooled by eight 4 mm diameter channels. In the central, coupler cell, RF probe is installed providing signal for RF system. The 1<sup>st</sup> orbit 10 MeV beam passes through 12 mm diameter hole drilled in the linac body.

To feed linac 2856 MHz, 6 MW/6 kW KIU-168 klystron is used [4]. Klystron operates in self-oscillation mode with accelerating structure in the feed-back loop similar to [5].

Two stainless steel welded vacuum chambers are mounted in the end magnet gaps. To avoid deformation of the chambers by atmospheric pressure the special spacers are inserted into the chamber. The chambers are connected by beam line tubes with the central vacuum chamber by bellow units. The whole system including the linac is pumped out through the central vacuum chamber (8) –Fig. 5 – and linac pumping port (6) by the ion pump (9).

## RTM STATUS

Now most of RTM elements (end magnets, an electron gun, injection and compensation magnets, quadrupole and solenoidal lenses, beam current monitors and steering coil units, end magnet vacuum chambers, a linac pumping port and bellow units, RTM frame) have been manufactured. To simplify RTM assembling and to provide several hundreds microns accuracy of the elements positioning with respect to median plane and linac axis, the RTM frame after welding was machined at a sufficiently long base.

RTM vacuum system elements: bellow units, linac pumping port, transition units with beam pipes and end magnet vacuum chambers have been tested for vacuum leakage and are ready for installation in RTM.

Before installation of the end magnets to the RTM frame the magnets were tested and tuned. To measure the end magnet median plane field distribution special stand for automated field measurements consisting of an adjustable magnet support, Hall probe movable in two directions, power supplies and a control computer was built. After end magnet tuning by adjustment the gap height between poles within several 10  $\mu\text{m}$  we obtained for both magnets the main pole field uniformity in the working region within 0.1% (seen in Fig.6) which corresponds to the project.

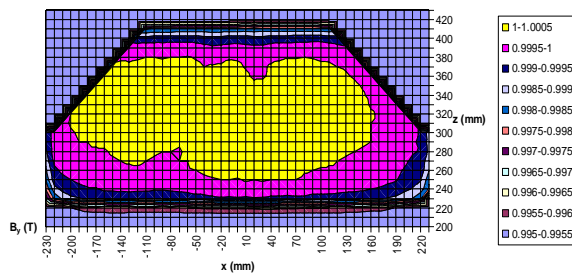


Figure 6: Median plane field distribution for the main pole region in the end magnet.

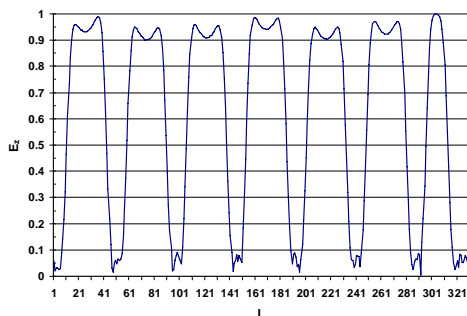


Figure 7: Distribution of electric field to axes of accelerating structure.

Manufactured linac segments (half-cells) were tested and tuned with a special stand including a network analyzer and a hydraulic press. In Fig. 7 we show measured on-axis electric field distribution before linac

brazing. Measured own quality factor before brazing is  $\sim 10800$ , coupling factor about 6.3% and linac-waveguide coupling coefficient  $\sim 2.5$ . The quality factor and both coupling coefficients will grow after linac brazing.

## CONCLUSION

Most of RTM elements have been manufactured and tested. Assemblage of the accelerator has been started as illustrated in Fig. 8.



Figure 8: RTM assembling.

## REFERENCES

- [1] A.I. Karev, A.A. Krasnov, I.S. Kuzmin, N.P. Sobenin, "Electrodynamics Calculations of the Accelerating Structure for 55 MeV Race-Track Microtron", Proceeding of the Scientific session MEPhI-2004, Moscow, vol.7, p.197 (2004).
- [2] A.A. Vetrov, A.I. Karev, I.S. Kuzmin, N.P. Sobenin, A.I. Fadin, "55 MeV Race-Track Microtron Beam Dynamics", Proceeding of the Scientific session MEPhI-2004, Moscow, vol.7, p.162 (2004).
- [3] V.G. Gevorkyan, A.B. Savitskiy, M.A. Sotnikov, V.I. Shvedunov, "Beam Dynamics Simulation Programs for Recirculating Accelerators: RTMTRACE", Moscow, Available from VINITI, 1989, no. 183-B89.
- [4] I.A. Frejdovich, P.V. Nevsky, V.P. Sakharov et al, Proceedings of the Seventh IEEE International Vacuum Electronics Conference and Sixth IEEE International Vacuum Electron Sources Conference, IVEC-IVESC 2006, April 25 – 27, 2006, Monterey, CA 93940, Report N13.5, 4 p.
- [5] A.N. Ermakov, D.I. Ermakov, B.S. Ishkhanov et al, An Injection and Acceleration System of a Pulsed Race-Track Microtron, Instruments and Experimental Techniques, Vol. 45, No. 4 (2002) 482–489